

Cluster models of the neutron and infrared vibrational spectra of vitreous silica

J. R. Banavar and J. C. Phillips

Bell Laboratories, Murray Hill, New Jersey 07974

(Received 24 January 1983)

Cluster models of g -SiO₂ were constructed. The neutron and infrared vibrational spectra of these clusters were calculated and found to be in good agreement with experiment. Our results show that certain strong and very narrow bands in the spectra of g -SiO₂ may be assigned to bonds associated with reconstructed bonds on the internal surfaces of paracrystalline clusters.

I. INTRODUCTION

Given the atomic positions, masses, and assumed interatomic forces of a set of atoms one can readily calculate the normal modes and their frequency spectrum by diagonalizing the equations of motion. With this information and with reasonable assumptions concerning neutron scattering lengths and effective atomic charges one can calculate as well the neutron scattering and infrared-absorption spectra. With considerably less confidence one can assume atom or bond polarizabilities and calculate the Raman spectra as well.

In crystals where the atomic positions and masses are known this program has often been adopted. With the interatomic forces and scattering strengths either calculated by other means or treated as adjustable parameters the comparison of theoretical and experimental spectra has often yielded substantial information concerning those forces and effective charges.¹

In this paper we shall be concerned with the vibrational spectra of the prototypical network glass, vitreous silica. In this case the atomic positions are not known and our primary aim is to determine certain characteristic properties of these positions by analyzing the spectra. Of course, we cannot invert the data to obtain the positions of all the atoms. At the same time certain characteristic properties of these positions (such as the radial distribution function) are probably best determined by other experiments (such as x-ray and neutron diffraction). In this example, because the angular information and the longer-range connectivity of the network are not contained in the data, relatively little can be learned about the structure of the network.

The vibrational spectra of nine models of vitreous silica, all with their atomic positions adjusted to produce radial distribution functions in good agreement with experiment, have been studied by Bell.² These models differ in the amount and degree of their topological disorder as reflected in their ring statistics. When the ring statistics are narrowly dispersed (e.g., in models with predominantly five- versus six-membered rings) the differences in vibrational spectra are quite pronounced. As the ring statistics broaden these differences are considerably reduced.

The general conclusion reached in an extensive series of papers by Bell, Dean, and others³⁻⁶ is that the vibrational

spectra of disordered network solids contain substantial structural information which complements the information contained in direct diffraction studies.⁷ Neither method is conclusive by itself, however, and considerable physical judgment, involving information obtained from still other sources, may be required to establish a plausible structural model.

Two examples of such other sources may be mentioned. The configurational entropy of vitreous silica is of order $0.4k_B$ /formula unit.⁸ Bell and Dean have shown⁹ that this amount of configurational entropy is consistent with the broad range of ring statistics assumed in their continuous random network model. However, they also show that the same configurational entropy can be obtained from a narrow distribution of ring statistics accompanied by about 5–10% broken bonds such as would be found on the surfaces of clusters (or microcrystallites) about 60 Å in diameter. The existence of such clusters in ultrathin drawn silica fibers not exposed to air, i.e., prepared and micrographed in high vacuum, has been observed directly by transmission-electron microscopy.¹⁰

The second example comes from the vibrational spectra themselves. The neutron vibrational spectrum of quartz SiO₂ is very similar to that of vitreous SiO₂, the latter being only a slightly broadened version of the former,¹¹ as shown for the reader's convenience in Figs. 1 and 2. The broadening here is comparable to the shifts that are observed¹² in the Raman scattering frequencies from bulk to microcrystalline silicon.

The characteristic feature that distinguishes cluster or microcrystalline models from monolithic or continuous random network (CRN) models is the presence of a high density of dangling or reconstructed bonds on the internal surfaces of the former. In a lengthy review¹³ of the experimental vibrational spectra of vitreous silica, germania, BeF₂, and many silicates and germanates, Phillips has recently suggested that certain strong and very narrow bands in the vibrational spectra of these tetrahedral glasses should be assigned to these surface bonds. The present calculations were undertaken to provide theoretical models which could complement his largely phenomenological analysis of the experimental spectra. The results of our calculations were in many respects both unexpected and unexpectedly informative. We feel that these calculations represent only the first step in extending

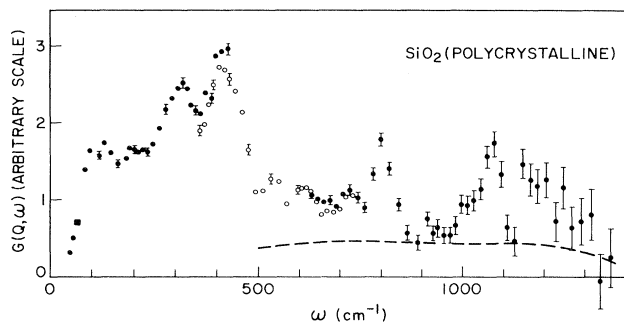


FIG. 1. Neutron scattering density of states $G(\omega)$ for crystalline quartz obtained by Leadbetter and Stringfellow (Ref. 11).

the concept of topological disorder to include pervasive internal surfaces, and that much still remains to be done to establish quantitatively the nature of interatomic forces at cluster surfaces. Overall, however, our results are consistent with the idea that some of the narrow bands in the vibrational spectra of these glasses are (internal) surface related.

II. CRN MODELS OF g -SiO₂

The basic model used in lattice-dynamical studies is one in which the atoms are treated as point objects undergoing small oscillations about their equilibrium positions. In the harmonic approximation, it is possible to find a unitary transformation to diagonalize the dynamical matrix. In their calculations, Bell and co-workers³⁻⁶ used an atomic model containing 188 SiO₄ units with 100 singly coordinated nonbridging oxygen atoms present on the model surface as (O_{1/2})₃-Si-O units. The surface units employed in their model violate the stoichiometry of the glass. Calculations of the spectra were carried out with two boundary conditions, fixed and free nonbridging oxygen atoms.

The force field employed nearest-neighbor interactions with both central- and non-central-force components. The atomic coordinates and interatomic forces were combined to obtain the elements of the dynamical matrix.

The distribution of eigenvalues was determined approximately by means of a theorem known as the negative-

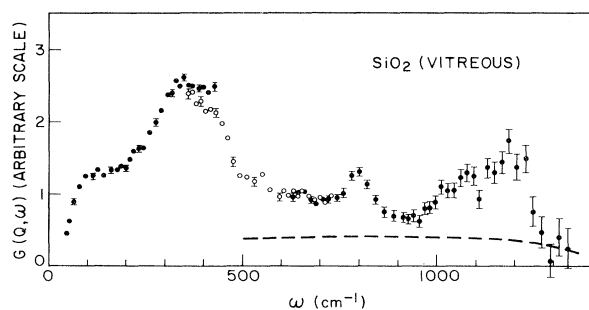


FIG. 2. Smoothed neutron scattering density of states $G(\omega)$ for g -SiO₂ as measured by Leadbetter and Stringfellow (Ref. 11).

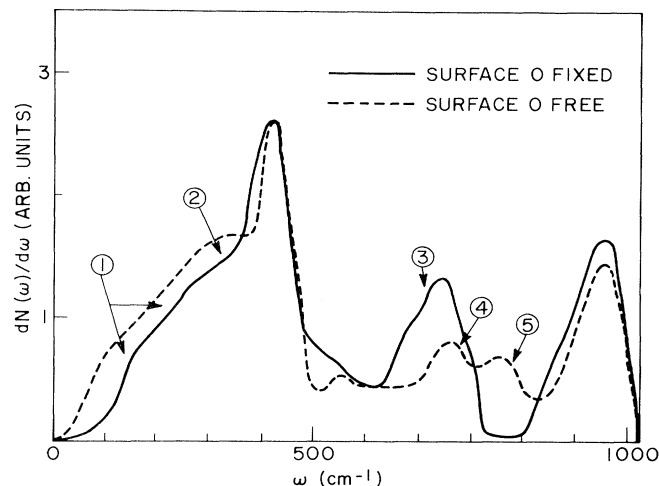


FIG. 3. Spectral densities $dN(\omega)/d\omega$ calculated by Bell *et al.* (Refs. 3-6) from their model for fixed and free surface O atoms. Following Phillips (Ref. 13) attention is drawn to (1) the downward shift or softening of the acoustic modes with free-surface atoms, (2) the weak localized resonance of the surface O-atom bending mode, (3) the upper cutoff peak of the $A_1 + E$ tetrahedral continuum for fixed-surface O atoms, (4) the same for free-surface O atoms, and (5) the localized modes of $A_1 + E$ surface molecules (O_{1/2})₃-Si-O for free-surface O atoms.

eigenvalue theorem.³ For obtaining the infrared spectrum a relatively small sample of typical eigenvectors were considered. The approximate numerical approach has the disadvantage that it does *not* yield information about the nature of low-frequency atomic vibrations below ~ 50 cm⁻¹. In practice most of the infrared and Raman spectra presented by Bell *et al.*⁵ are cut off below 200 cm⁻¹.

The calculations of the vibrational spectra provide information about the local modes associated with the (O_{1/2})₃-Si-O surface molecules (Fig. 3). In the free-end model, the acoustic-mode spectral density is shifted down-

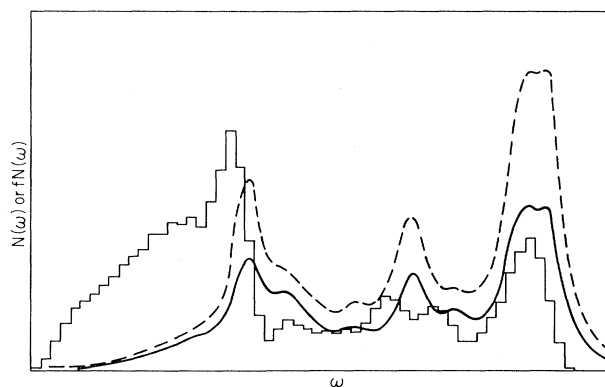


FIG. 4. Frequency and absorption spectra for vitreous SiO₂ calculated with free-surface O atoms by Bell *et al.* (Ref. 5). Continuous and broken curves correspond to different choices of the effective charge parameters. Histogram shows the frequency spectrum.

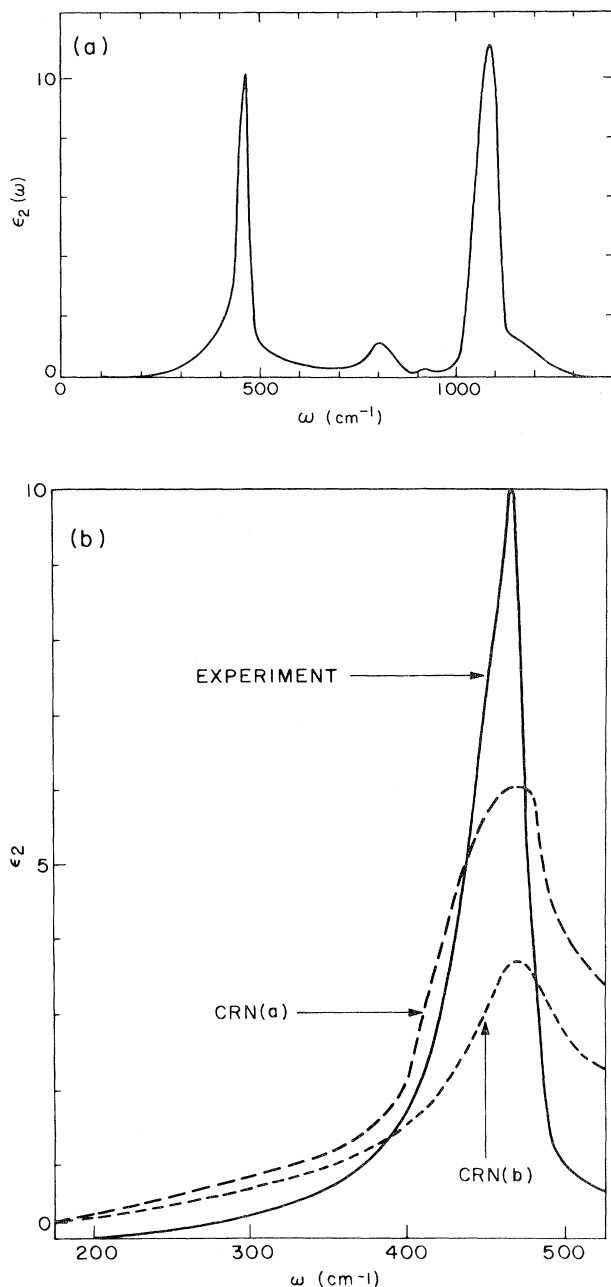


FIG. 5. (a) Absorptive part $\epsilon_2 = 2nk$ of the dielectric constant as a function of frequency ω . Data were obtained by Gaskell and Johnson (Ref. 14). (b) Absorptive part ϵ_2 of the dielectric constant as a function of frequency ω . Experimental peak at 460 cm^{-1} is very narrow with a full width at half maximum (FWHM) of 40 cm^{-1} (data from Ref. 14). Theoretical calculations with different effective charges are based on CRN models (from Ref. 5).

ward by about 50 cm^{-1} from the fixed-end spectrum. The localized modes are, to a large extent, found to be mixed in with the acoustic continuum. This is due in part to the fact that Bell *et al.* employ single-bond force constants for their nonbridging oxygen atoms.

We now turn to an analysis of the infrared-absorption spectrum calculated by Bell and Hibbins-Butler (Fig. 4).⁵ For comparison, the experimental infrared-absorption spectrum obtained by Gaskell and Johnson¹⁴ is shown in Figs. 5(a) and 5(b). The peak frequency (470 cm^{-1}) is in very good accord with experiment (460 cm^{-1}). The width of the peak is, however, too large and at $\omega = 200 \text{ cm}^{-1}$, the absorption is about an order of magnitude larger than that observed experimentally.¹⁴ This large inhomogeneous broadening could well be due to the wide dispersion in ring statistics.

III. MECHANICAL MODEL

A. Cluster geometry

The clusters were chosen to have the morphology of the high-temperature phase of crystalline SiO_2 , i.e., β -cristobalite. The crystalline structure¹⁵ is that of the cubic Si crystal with oxygen atoms statistically distributed, one oxygen atom in one of six equivalent sites clustered around the midpoint of the line joining two silicon nearest neighbors (Fig. 6). For simplicity, however, we let the oxygen atoms lie randomly on the circle shown in Fig. 6, such that the Si—O—Si angle was $\sim 147^\circ$, i.e., the allowed points were increased from six to infinity.

Starting with one of the oxygen atoms as the origin, concentric spheres were drawn to enclose all silicon atoms within a given distance from the origin. Five such clusters were constructed, the smallest containing two silicon atoms, while the largest had 38 silicon atoms. Table I lists

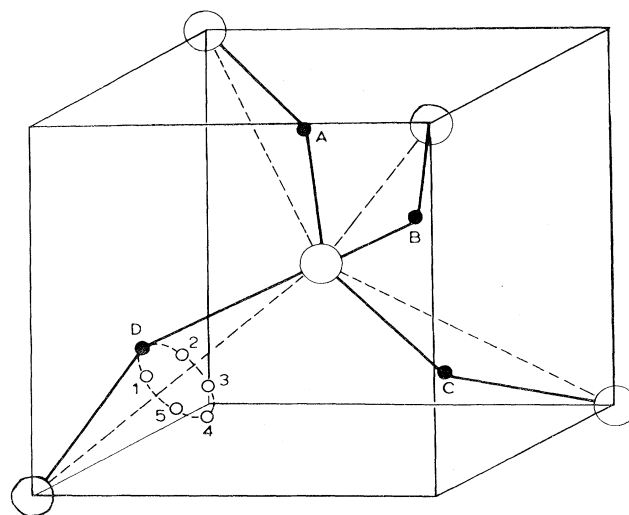


FIG. 6. Local atomic arrangements in cristobalite [after Wright and Leadbetter (Ref. 15)]. Large open circles represent silicon atoms and small solid circles denote oxygen atoms occupying one of six alternative positions displaced from the ideal position centered on the Si-Si axis. Small open circles represent the other possible oxygen positions around one Si-Si axis. In the present paracrystalline cluster models the oxygen atoms were allowed to lie randomly anywhere on the dashed circle.

TABLE I. Number of different kinds of atoms in each of the five clusters of SiO₂ and in the model of Bell *et al.* (Ref. 4).

	No. of Si atoms	No. of O atoms	No. of O _S [*] atoms
Cluster 1	2	4	3
Cluster 2	8	16	9
Cluster 3	20	40	15
Cluster 4	32	64	21
Cluster 5	38	76	21
BD Model	188	426	100

the numbers of different kinds of atoms in each of the five clusters and, for comparison, in the model of Bell *et al.*⁴ The number of surface oxygen atoms was chosen to preserve the stoichiometry and wherever possible these O_S^{*} atoms were double bonded to the silicon atoms at the edge of the cluster in nearly equivalent O_S^{*}=Si-(O_{1/2})₂ configurations. The Si=O_S^{*} double bond was chosen to point radially out from the cluster center. The bond length for the double bond connecting the nonbridging O_S^{*} atom to Si was chosen to be 90% of the single bond length in the bulk of the cluster. The number of O_S^{*} atoms was three in the smallest cluster and 21 in the largest cluster studied. The largest cluster had 114 atoms and was large enough to distinguish the normal modes that were internal to the cluster and bulklike from the modes localized near the cluster surface.

B. Force constants

A three-force-constant model was used to describe the interatomic forces. Valence-force fields were used rather than central forces in order to guarantee rotational and translational invariance. This resulted in vibrational spectra which always contained six zeros, consistent with free-boundary conditions. The interactions were determined by starting with those for molecular SiF₄ and by scaling them and adding a third interaction. The bond-stretching force constant for Si-O in the interior of the cluster was chosen to be 550 N/m. The corresponding force constant for the Si=O_S^{*} bond was chosen to be 25% larger consistent with the force-constant scaling $K \propto r^{-2.5}$. The bond-bending force constants for O-Si-O and Si-O-Si were chosen to be 7.7×10^{-19} and 2.6×10^{-18} J, respectively (note that the ratio of the equilibrium O-Si-O and Si-O-Si angles is about 0.75).

To simulate the interaction of the cluster with the surrounding clusters, the diagonal elements of the potential-energy matrix corresponding to the O_S^{*} atoms were incremented by $\omega_0^2 = (350 \text{ cm}^{-1})^2$. This interaction fixes the cluster and causes the disappearance of the six zero-frequency vibrational modes as well as strengthens the intracluster surface modes.

C. Vibrational and infrared spectra

The dynamical matrix was obtained and was diagonalized *exactly* and all eigenvalues and eigenvectors were

determined. This enabled us to obtain information about low-lying modes which Bell and co-workers³⁻⁶ were unable to get using their approximate diagonalization scheme. As discussed in the next section a study of the low-frequency modes shows the importance of the intercluster interactions of a pervasive (percolative) nature in stabilizing the surface modes.

The infrared spectra were calculated using the point-charge model. The absorption coefficient of the vibrating solid has the general form

$$F(\omega) = g(\omega)R(\omega), \quad (1)$$

where $g(\omega)$ is the vibrational density of states and $R(\omega)$ is a function which describes the strength of the coupling between the incident infrared radiation and the vibrational modes of frequency ω .

In the point-charge model we assign charges of +4 and -2 to the silicon and oxygen atoms, respectively. For such a model, the dipole-moment derivative is given by

$$\bar{\mu}(\omega) = \sum_j q_j \bar{x}_j(\omega), \quad (2)$$

where q_j is the charge of the j th atom and $x_j(\omega)$ denotes an eigenmode of the vibrational spectrum with frequency ω . The response function $R(\omega)$ is then proportional to $|\bar{\mu}(\omega)|^2$.

D. Comparison of the cluster model with the CRN model of Bell *et al.* (the BD model)

For the reader's convenience we have compiled a brief guide which summarizes the key differences between our model and the model of Bell *et al.*³⁻⁶ which has long been recognized as the standard work in this field. These differences are the following.

(1) The cluster model has an interior with the morphology of β -cristobalite. The BD model, on the other hand, is a CRN.

(2) The surface of the cluster model is covered with O_S^{*} atoms in the trigonal configuration (O_{1/2})₂-Si=O_S^{*}, whereas the surface of the BD model has O_S^{*} atoms in the tetrahedral configuration (O_{1/2})₃-Si-O_S^{*}.

(3) In the cluster model, the O_S^{*} atoms, in addition to being coupled to the atoms within the cluster, have an interaction simulating the intercluster interactions. In the BD model, the O_S^{*} atoms were either allowed to be free or were held fixed, corresponding to zero or infinite intercluster interactions, respectively.

(4) In the cluster model the Si=O_S^{*} bond-stretching interaction is 25% larger than the Si-O interaction in the interior of the cluster, whereas the Si-O interaction is taken to be the same both in the bulk and at the surface in the BD model.

(5) The ring statistics in the cluster model are dominated by six (cation-O)-membered rings, whereas in the BD model there is substantial inhomogeneous ring disorder.

(6) The cluster model satisfies the SiO₂ stoichiometry, whereas the BD model does not. In particular, while using the point-charge model to calculate the infrared spectrum, this leads to violation of charge neutrality in

the BD model.

(7) The dynamical matrix is diagonalized exactly in the present calculation, whereas the BD calculation used approximate methods for determining some selected eigenvalues and eigenvectors. In particular, their scheme does not permit a study of the low-frequency eigenmodes.

IV. RESULTS

A. Vibrational spectrum

We begin by noting that in an isolated cluster, the surface modes are not dynamically so stable as they would be when the intercluster interactions are taken into account. We carried out the calculations for two kinds of clusters. In the first case, the bulk oxygen atoms were allowed to lie on the straight line joining nearest-neighbor Si atoms (the Si—O—Si angle was 180°). For such clusters, when only nearest- and next-nearest-neighbor central forces are assumed (the bond-bending interactions are taken to be zero), we found that for four of the five clusters there were $3N_S$ zero-frequency vibrational modes, where N_S refers to the number of O_S^* atoms. These marginally stable eigenmodes appeared to be extended throughout the cluster. On allowing the bulk oxygen atoms to buckle, so that the Si—O—S angle was $\sim 147^\circ$, some of the modes moved up to a nonzero, albeit small, frequency. Upon further turning on the bond-bending interactions, the degeneracy was lifted and while six of the modes had zero

frequency, the remaining $(3N_S - 6)$ were still low-lying modes with more than half of them lying below 50 cm^{-1} .

One might imagine, from the trigonal symmetry of the $(O_{1/2})_2\text{—Si=O}_S^*$ surface units, that the O_S^* vibrations normal to the plane of these units would be marginally stable. There are, however, only N_S surface modes of this type. This leaves the existence of $3N_S$ marginally stable surface modes unexplained. For our physical model of $g\text{-SiO}_2$ this instability is removed (see below) by intercluster interactions. However, for the isolated cluster, regarded merely as a mathematical model, the existence of so many marginally stable modes is a puzzle which we have resolved with the assistance of Thorpe¹⁶ and Weaire.¹⁶ One can show that in the unbuckled or collinear Si—O—Si geometry the Si—Si central second-neighbor force constraints are ineffective because of collinearity. When one then counts the total number of remaining constraints per formula unit one finds that in the bulk the numbers of constraints and degrees of freedom are equal. At the surface, however, one finds a constraint deficiency which is just $3N_S$ if the $(O_{1/2})_2\text{—Si=O}_S^*$ units are not coplanar and $4N_S$ if they are. This constraint-counting prescription describes our results exactly in the unbuckled or collinear geometry.

Returning to the problem at hand, we feel that in $g\text{-SiO}_2$ the basic physics is that there are many snugly embedded clusters and it is the cluster-cluster interaction that strengthens the low-lying intracluster surface modes. We have attempted to simulate the intercluster interactions as

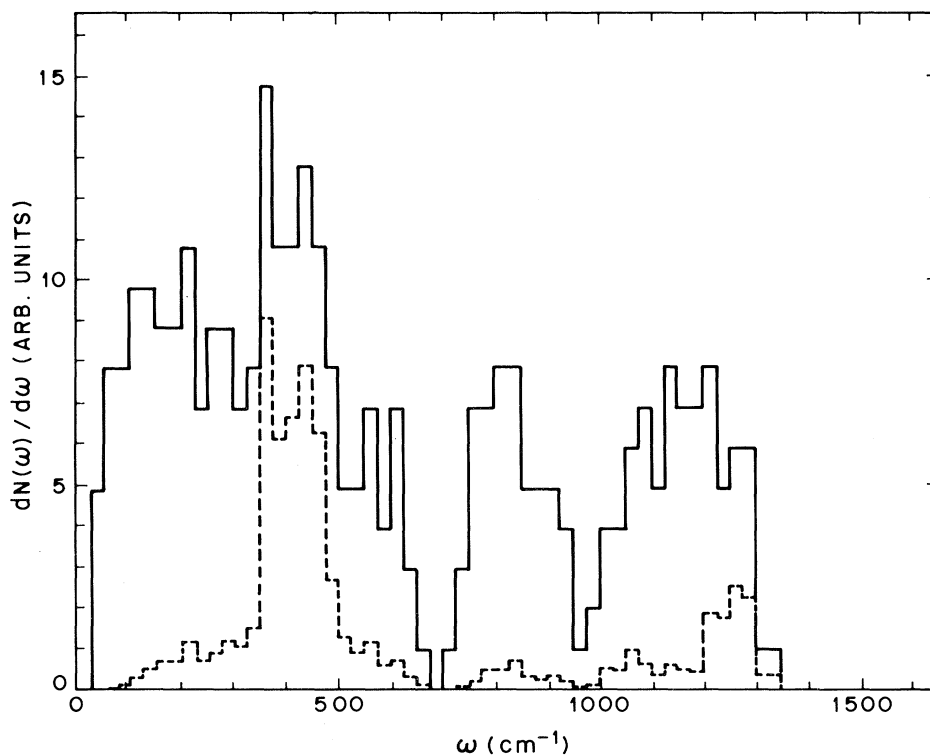


FIG. 7. Solid line gives the total spectral density $dN(\omega)/d\omega$ calculated for the largest cluster (see Table I), while the dashed line represents part of this density obtained by projection on the O_S^* surface atoms.

described in Sec. III.

Qualitatively similar results were obtained for clusters of different sizes. Figure 7 shows the histogram of the vibrational density of states $g(\omega)$ for the largest cluster.

The spectral density associated with the nonbridging surface oxygen atoms is shown as a separate contribution. The results are in good quantitative agreement with the neutron scattering measurements of Leadbetter and Stringfellow.¹¹ The three-peak structure is reproduced by our calculations. The surface contributions occur primarily in the $F_2^{1,2}$ bands (the first and third peaks in the vibrational density of states). Since the surface molecules $(O_{1/2})_2-Si=O$ are trigonal and not tetrahedral, we do not find a localized surface mode associated with the cutoff of the A_1+E tetrahedral band¹³ around 800 cm^{-1} . The position of this band is found to depend sensitively on the strength of the $Si-O-Si$ bond-bending interaction. (For example, if this weak interaction is reduced to zero, the trough between the 400 - and 800-cm^{-1} peaks nearly disappears.) Our results are consistent with the suggestion¹³ that the satellite peak at 410 cm^{-1} in the neutron scattering data is associated with the intracuster surface modes with the frequency determined primarily by the strength of the intercluster interactions.

B. Infrared spectrum

The infrared spectrum for the largest cluster calculated using the point-charge approximation is shown in Fig. 8.

Our results are again good in agreement with those obtained by Gaskell and Johnson¹⁴ (Fig. 5) with a few notable exceptions. In our calculation the intercluster interactions have been treated approximately by strengthening the diagonal elements in the dynamical matrix corresponding to the O_S^* atoms. A fundamental shortcoming of the present work is that we have not allowed for relaxation of the O_S^* atoms. This leads to two spurious features in the spectrum, the bump in the $(0-100)\text{-cm}^{-1}$ range and the double-peak structure around 400 cm^{-1} .

The first of the double peaks occurs at 350 cm^{-1} , the value chosen for the intercluster interaction, whereas the second peak occurs at a somewhat higher value. Smearing out the intercluster interaction randomly around 350 cm^{-1} leads to a broader diffuse peak. Apart from the existence of the double peak, the absorption does fall off quickly (quite possibly exponentially) with decreasing frequency in qualitative agreement with experiment.¹⁴ A systematic study of the double-peak sizes as a function of the cluster size leads us to believe that the effect is not due to the finite size of the cluster, but that it may be associated with splitting of the transverse O_S^* modes parallel or perpendicular to the $(O_{1/2})_2-Si=O_S^*$ plane. It seems likely that the effect may disappear on fully relaxing the O_S^* atoms taking into account their interactions with both atoms within the cluster and atoms in the neighboring clusters.

We note that the force constants were adjusted while calculating the vibrational density of states $N(\omega)$ so that

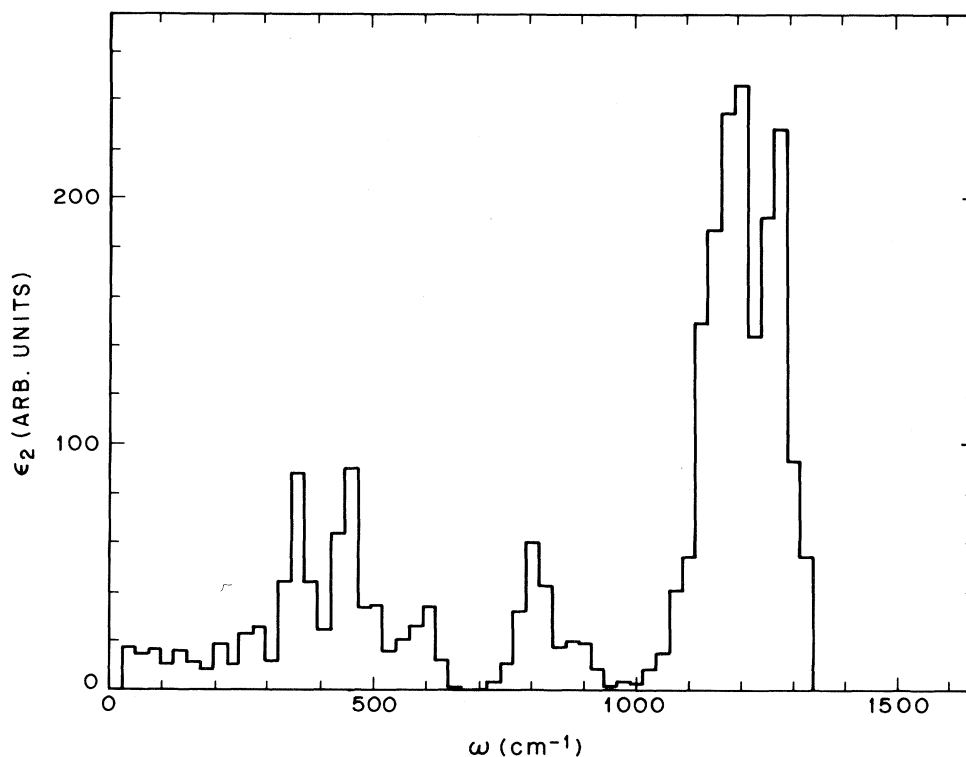


FIG. 8. Absorption spectrum calculated for the largest cluster (see Table I).

some of the good agreement for that spectrum arises by construction. However, no further adjustment was made while obtaining the infrared spectrum. The fundamental difference between the model of Bell *et al.*⁴ and the cluster model is that whereas in the former case one gets a wide peak in the infrared spectrum, a narrow surface band is obtained in the cluster model. In fact, on very general grounds, a mode localized at the surface would be expected to decay exponentially as one goes into the interior of a paracrystalline cluster. The rapid (possibly exponential) decay of the infrared-absorption spectrum is, in fact, found to be a general feature of the present paracrystalline cluster models independent of the nature of the force constants used. Again the reader should note that whereas Bell *et al.* obtain good agreement for $N(\omega)$ and poor agreement for the infrared spectrum our model agrees with experiment equally well for both cases.

V. CONCLUSION

In this paper, we have studied the neutron and infrared vibrational spectra of a prototypical network glass $g\text{-SiO}_2$. In contrast to the studies by Bell and co-workers³⁻⁶ of the CRN models, we have carried out, for the first time, analogous calculations based on a chemically plausible cluster or microcrystalline model. Our results strongly support an earlier suggestion of Phillips¹³ that certain strong and narrow bands in the vibrational spectra of $g\text{-SiO}_2$ should be assigned to bands associated with reconstructed bands on the internal surfaces of the microcrystalline model. In particular, our results are consistent with the suggestion that the satellite peak at 410 cm^{-1} in the neutron scattering data is associated with the intra-cluster surface modes with its frequency determined mainly by the strength of the cluster-cluster interactions.

One surprising feature of our calculations was the discovery of certain hidden symmetries which are exact when only central-force interactions are present in the cluster and the bulk oxygen atoms lie on the straight line joining nearest-neighbor silicon atoms. For clusters having N_S surface oxygen atoms, these lead to $3N_S$ marginally stable zero-frequency vibrational modes. It is important to realize that the identification of these cyclical modes is nontrivial. For example, our surface-based cyclical modes in the presence of first- and second-neighbor central forces should not be confused with the trivial bulk cyclical modes which can be found in non-close-packed infinite lattices (e.g., simple cubic, diamond, bcc, etc.) with

first-neighbor central forces only.

In conclusion, we feel that these calculations are only the first steps in studying the effects of topological disorder caused by percolative internal surfaces on the vibrational spectra of network glasses. While our results show the important role played by these internal surfaces in causing the strong narrow bands in the spectra, a full understanding of the atomic interactions at cluster surfaces must await further work.

Note added

After this paper was submitted for publication, Magaña and Lannin¹⁷ reported an important Raman scattering experiment on liquid GeSe_2 . They found that the frequencies of the A_1 and companion A_{1c} Raman bands in the glass are both relaxed in the liquid, but by different amounts. According to earlier analysis¹⁸ the A_1 breathing mode is associated with tetrahedra in the interior of a $\text{Ge}_{22}\text{Se}_{46}$ raftlike cluster, while the A_{1c} mode is associated with tetrahedra at the edges of the cluster. Magaña and Lannin found a 3% relaxation of the interior A_1 modes and a 5% relaxation of the A_{1c} modes. The cluster analysis of Aronovitz *et al.* of these rafts showed¹⁸ that approximately 10% of the A_{1c} frequency arises from intercluster forces, so that an additional 2% relaxation of the A_{1c} mode compared to the A_1 mode is traceable to a 20% reduction in the intercluster forces in the supercooled liquid compared to the glass.

In the cristobalite geometry we have seen that almost all of the restoring force for the surface modes comes from intercluster interactions. It would therefore appear that a very large infrared shift of surface-related modes should be observable by melting $g\text{-SiO}_2$. Indeed, if the 490-cm^{-1} mode is a surface mode, a reduction of frequency of order $50\text{--}100\text{ cm}^{-1}$ should be observed, according to our model, with relatively little reduction in Raman scattering strength. Other models (which assign the 490-cm^{-1} line to four-membered planar rings, for example¹⁹) would apparently predict either no change in the line upon melting, or a reduction of its strength (if the small rings melt) or an increase in its strength (if the temperature increase produces an increase in the small-ring population). All these predictions are qualitatively different and only the present model predicts a strong infrared shift. This shift could also be accompanied by broadening and an apparent loss of scattering strength, but the infrared shift should still be observable. It is hoped that high-temperature studies of the Raman spectra of $g\text{-SiO}_2$ by Walrafen, currently in progress, will resolve this problem.

¹S. S. Mitra, *Solid State Physics* (Academic, New York, 1962), Vol. 13, p. 1.

²R. J. Bell, *J. Phys. C* **7**, L265 (1974).

³R. J. Bell, N. F. Bird, and P. Dean, *J. Phys. C* **1**, 299 (1968); **7**, 2547 (1974); R. J. Bell, *ibid.* **5**, L315 (1972); P. Dean, *Rev. Mod. Phys.* **44**, 127 (1972).

⁴R. J. Bell and P. Dean, *Nature* **212**, 1354 (1966); *Philos. Mag.* **25**, 1381 (1972); R. J. Bell, *Methods Comput. Phys.* **15**, 216 (1976).

⁵R. J. Bell and D. C. Hibbins-Butler, *J. Phys. C* **9**, 2955 (1976);

9, 1171 (1976); **8**, 787 (1975).

⁶R. J. Bell, P. Dean, and D. C. Hibbins-Butler, *J. Phys. C* **3**, 2111 (1970); **4**, 1214 (1971).

⁷R. L. Mozzi and B. E. Warren, *J. Appl. Cryst.* **2**, 164 (1969); J. R. G. Da Silva, D. G. Pinatti, C. E. Anderson, and M. L. Rudee, *Philos. Mag.* **31**, 713 (1975).

⁸I. Gutzow, *Z. Phys. Chem.* **221**, 153 (1962).

⁹R. J. Bell and P. Dean, *Phys. Chem. Glass.* **9**, 125 (1968).

¹⁰J. Zarzycki and R. Mezard, *Phys. Chem. Glass.* **3**, 163 (1962); J. Zarzycki, *C. R. Acad. Sci. (Paris) B* **271**, 242 (1970).

- ¹¹A. J. Leadbetter and M. W. Stringfellow, in *Neutron Inelastic Scattering: Proceedings of the Grenoble Conference, 1972*, (IAEA, Vienna, 1974), p. 501; see also F. L. Galeener, A. J. Leadbetter, and M. W. Stringfellow, *Phys. Rev. B* 27, 1052 (1983).
- ¹²S. Vepřek, Z. Iqbal, H. R. Oswald, and A. P. Webb, *J. Phys. C* 14, 295 (1981).
- ¹³J. C. Phillips, *Solid State Physics* (Academic, New York, 1982), Vol. 37, p. 93.
- ¹⁴P. H. Gaskell and D. W. Johnson, *J. Non-Cryst. Solids* 20, 153 (1976); 20, 171 (1976).
- ¹⁵A. F. Wright and A. J. Leadbetter, *Philos. Mag.* 31, 1391 (1975).
- ¹⁶M. F. Thorpe (private communication); D. Weaire (private communication).
- ¹⁷J. R. Magaña and J. S. Lannin, *Bull. Am. Phys. Soc.* 28, 328 (1983).
- ¹⁸P. M. Bridenbaugh, G. P. Espinosa, J. E. Griffiths, J. C. Phillips, and J. P. Remeika, *Phys. Rev. B* 20, 4140 (1979); P. Boolchand, J. Grothaus, and J. C. Phillips, *Solid State Commun.* 45, 183 (1983); J. A. Aronovitz, J. R. Banavar, M. A. Marcus, and J. C. Phillips (unpublished).
- ¹⁹F. L. Galeener, *Solid State Commun.* 44, 1037 (1982).